

Control of the acoustic waves generated by intense laser filamentation in water

V. Jukna, S. Albert, C. Millon, Benoît Mahieu, R. Guillermin, G. Rabau, D. Fattaccioli, André Mysyrowicz, A. Couairon, Aurélien Houard

▶ **To cite this version:**

V. Jukna, S. Albert, C. Millon, Benoît Mahieu, R. Guillermin, et al.. Control of the acoustic waves generated by intense laser filamentation in water. Optics Express, 2022, 30 (6), pp.9103-9111. 10.1364/OE.453749 . hal-03600542

HAL Id: hal-03600542

https://ensta-paris.hal.science/hal-03600542

Submitted on 7 Mar 2022

HAL is a multi-disciplinary open access archive for the deposit and dissemination of scientific research documents, whether they are published or not. The documents may come from teaching and research institutions in France or abroad, or from public or private research centers.

L'archive ouverte pluridisciplinaire **HAL**, est destinée au dépôt et à la diffusion de documents scientifiques de niveau recherche, publiés ou non, émanant des établissements d'enseignement et de recherche français ou étrangers, des laboratoires publics ou privés.



Distributed under a Creative Commons Attribution 4.0 International License

Research Article Vol. 30, No. 6 / 14 Mar 2022 / Optics Express 9103
Optics EXPRESS

Control of the acoustic waves generated by intense laser filamentation in water

V. Jukna,[1,2,3] S. Albert,[1] C. Millon,[1] B. Mahieu,[1] R. Guillermin,[4] G. Rabau,[4] D. Fattaccioli,[5] A. Mysyrowicz,[1] A. Couairon,[2] and A. Houard[1,*]

[1]LOA, ENSTA Paris, CNRS, Ecole polytechnique, Institut polytechnique de Paris, 828 bd des Maréchaux, 91762 Palaiseau, France
[2]Centre de Physique Théorique, CNRS, Ecole polytechnique, Institut polytechnique de Paris, F-91128 Palaiseau, France
[3]Laser Research Center, Vilnius University, Saulėtekio Avenue 10, LT, 10223 Vilnius, Lithuania
[4]Laboratoire de Mécanique et d'Acoustique, UMR 7031, CNRS, Aix Marseille Univ, Centrale Marseille, 4 impasse Nikola Tesla, Marseille, France
[5]DGA Techniques Navales, Toulon, France
*aurelien.houard@ensta-paris.fr

Abstract: Experiments and simulations are performed to study filamentation and generation of acoustic waves in water by loosely focused multi-millijoules laser pulses. When the laser pulse duration is increased from femtosecond to nanosecond duration, a transition is observed from a filamentary propagation with extended and low energy density deposition to a localized breakdown, related to high energy density deposition. The transition suggests that Kerr self-focusing plays a major role in the beam propagation dynamics. As a result, the shape, the amplitude and the spectrum of the resulting pressure wave present a strong dependence on the laser pulse duration.

© 2022 Optica Publishing Group under the terms of the Optica Open Access Publishing Agreement

1. Introduction

Laser-induced energy deposition in water and hydrodynamic effects following optical breakdown have been investigated for the past decades with different types of laser sources [1–5]. At short distance laser-induced acoustic sources could open up new possibilities for high resolution imaging and tomography in the ultrasound domain [6–9], while long distance generation of plasmas emitting in the sonar range could be used for underwater communications, and fast characterization of marine environment [10–11]. The process of laser induced acoustic waves is well known for nanosecond laser pulse tightly focused in water. When the laser intensity at the focus is high enough, multi-photon and avalanche ionization will produce material breakdown. The deposited energy rapidly transforms into heating of the material and generates a cavitation bubble and consequently a spherical pressure wave [12]. The amplitude of this pressure wave can depend on the laser pulse duration [5]. Also, in transparent solids, the efficiency of plasma generation and laser interaction with material has been investigated by many groups, because of its paramount importance in laser induced damage [13] and micromachining [14]. It was observed that pulses of longer duration and fluence above damage threshold generate stronger shockwaves, higher plasma densities and voids. In the case of bulk micromachining of glasses, shorter pulses tend to change the refractive index of the material while longer pulses generate voids [15–16].

The recent development of intense ultrashort laser sources based on chirped pulse amplification [17], with high peak power and high repetition rate [18–19] has raised new perspectives for laser induced acoustics in water [4,20–21]. In the case of a femtosecond laser pulse having a peak power larger than the critical power for self-focusing (P_{cr}~4 MW in water for a pulse at 800 nm),

#453749 https://doi.org/10.1364/OE.453749
Journal © 2022 Received 13 Jan 2022; revised 23 Feb 2022; accepted 23 Feb 2022; published 3 Mar 2022

Optics EXPRESS

the laser will generate light filaments, or undergo multifilamentation if the peak power largely exceeds P_{cr} and even produce a superfilament if the beam is focused [21–23]. A long track of plasma is produced in the wake of these filaments and initiates a cylindrical shock wave traveling perpendicular to the track. Due to the elongation of the emitter, the directivity of the pressure wave is enhanced [4]. The broad spectrum of femtosecond pulses can also be exploited to obtain temporal focusing of the pulse at a remote location, by applying an initial negative chirp [11].

In this article we characterize in detail the pressure wave produced by loosely focused multi-millijoule laser pulses in water. We investigate the influence of laser pulse duration and energy on the generation of pressure wave. The strength of the pressure wave is characterized with hydrophones in the frequency range between 0.1 Hz and 20 MHz, while the evolution of the pressure wave is measured using time resolved Schlieren imaging. The shape, the amplitude and the spectrum of the resulting pressure wave present a strong dependence on the laser pulse duration. A dependence of the acoustic wave features on the laser repetition rate is also observed, and seems related to the dynamics of the cavitation bubbles created by the laser.

2. Experimental setup

The experimental setup is depicted in Fig. 1(a). Two distinct pump laser sources were used in order to increase the range of investigated pulse duration. The first one is a chirped-pulse amplified Ti:Sapphire laser chain, delivering pulses with a central wavelength of 800 nm, and a pulse duration that can be tuned from 50 fs (transform limited pulse) to 16 ps by introducing a linear chirp. The initial laser beam diameter is 35 mm FWHM, but is reduced to 20 mm with an adjustable iris. The laser beam energy was measured after the iris and was adjustable between 1 and 16 mJ. For this laser, the pulse energy is high enough to generate superfilaments in water as the ratio between the peak power P and the critical power for self-focusing P_{cr} ($N = P/P_{cr}$ where $P_{cr} = 3.8$ MW) varies from 98 000 for a 50-fs pulse to 250 for a 16-ps pulse. The second pump laser source is a Nd:YAG laser delivering 10 ns pulses at 532 nm, with an energy up to 100 mJ with 20 mm FWHM beam diameter. In both cases the laser beam was focused in water by a 200 mm focal length lens placed 10 cm away from the water cell, corresponding to a numerical aperture of 0.06 in water. The repetition rate was initially set to 0.1 Hz. To characterize the pressure waves generated by the laser pulses, three different hydrophones were simultaneously used to cover the 0.1 Hz - 20 MHz frequency range: a Brüel & Kjaer hydrophone type 8103 for the low frequencies (0.1 Hz-180 kHz), a Reson model TC4035 for the middle frequency range (10 kHz-800 kHz) and a Precision Acoustics 1 mm needle hydrophone for the high frequencies (1 MHz -20 MHz). The hydrophones were positioned 7.7 cm away from the beam focus in the transverse direction with respect to the laser beam propagation axis (see Fig. 1). Additionally,

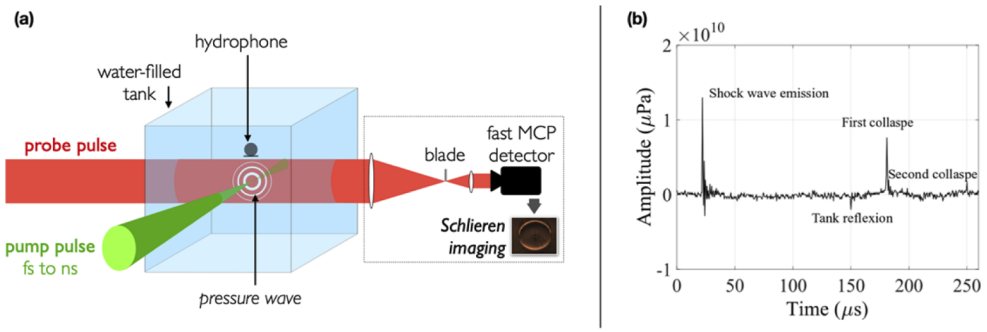


Fig. 1. (a) Experimental setup. (b) Example of an acoustic signal received with the high frequency hydrophone.

Optics EXPRESS

time-resolved Schlieren imaging of the shock wave was performed by means of a low-intensity probe laser with a 50 ns pulse duration (Cavitar Cavilux HF laser diode @ 630 nm) coupled with a fast microchannel plate (MCP) detector and electronically triggered by the delay generator of the laser system.

3. Experimental characterization of the laser generated pressure wave

3.1. Acoustic signal and spectrum of the pressure wave

The signals collected by each hydrophone were deconvoluted by the spectral response of the hydrophone to retrieve a pressure wave signal in µPa. An example of pressure signal detected by the high frequency hydrophone is presented in Fig. 1(b) in the case of a 6-mJ nanosecond laser pump pulse. The signal presents three distinct positive peaks with µs duration. This multiple pressure wave emission is due to the repetitive cavitation of the bubble formed, as described in [24]. The first peak corresponds to the initial pressure wave emitted by the laser induced breakdown of water. After the emission of this shockwave a cavitation bubble forms and rapidly grows, reducing the temperature of the gas inside. When the pressure inside the bubble becomes lower than the surrounding pressure, the bubble undergoes size contraction and then collapses after a few 100 µs. A second shockwave is then emitted as observed in the signal and finally, provided the system has enough energy left, another oscillation of the bubble may occur and emit a third pressure peak. We have confirmed in a smaller water cell that the resurgences of the shockwave are indeed correlated with multiple collapses of the cavitation bubble. We also observed that the delay between the two pressure peaks increases with the increase of initial pulse energy. This indicates that a larger bubble is generated. Calculations based on the Rayleigh-Plesset equation allow us to give a rough estimation of the cavitation bubble radius of 1 mm for a pulse of 10 ns duration and 6.3 mJ energy [25]. In the following analysis, we will concentrate on the first peak and use averaged signal to increase the signal/noise ratio. Since the delays of the secondary peaks vary a lot from shot to shot, they disappear in the averaged signal.

Figure 2 presents the retrieved pressure wave spectra for three typical pulse durations and for an input pulse energy of 7 mJ. One can see that the spectrum of the pressure signal is particularly broad and extends from 5 kHz to 4 MHz. Moreover, the acoustic amplitude is increased by several orders of magnitude as the pulse duration goes from 700 fs to 10 ns. The spectral shape also strongly depends on the laser pulse duration. While femtosecond pulses generate a signal with a pronounced peak at 2 MHz, the spectrum produced by the 15 ps and the 10 ns pulse are almost flat below 1 MHz. Therefore, longer laser pulses are more suitable for long distance underwater applications, where kHz frequencies are usually employed because of their low absorption in water. In addition, the level of the acoustic signal produced in the kHz range by the nanosecond laser is comparable to the one produce by a sonar (about 200 dB ref 1µPa at 1 m [26]).

3.2. Dependence on the laser pulse energy

First, we measured the evolution of the sound wave amplitude as a function of the laser input energy. With a pulse at 800 nm of a few mJ of energy, we were not able to detect sound waves for laser pulse durations shorter than 600 fs. The signal amplitude dependences on pulse energy for pulse durations of 670 fs, 8 ps, 15 ps and 7 ns are plotted in Fig. 3. Above 0.5 mJ the amplitude of the pressure wave quickly increases with the increase of laser energy and starts to saturate above 4 mJ. This increase is particularly fast for ps and ns pulses, and can be explained by avalanche ionization. We interpret the saturation observed with long pulses as been due to the formation of an overcritical plasma density that diffracts the pulse. Results also confirm that longer pulse durations generate higher amplitude sound waves. For the nanosecond laser, the acoustic signal amplitude is 13 to 21 dB larger than for a 15 ps pulse of similar energy.

Optics EXPRESS

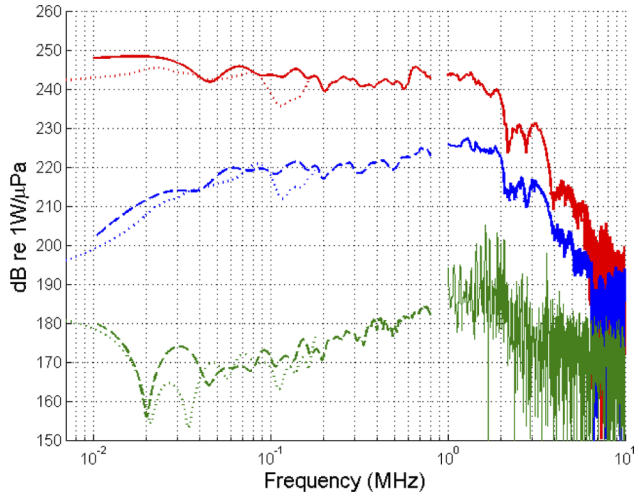


Fig. 2. Spectrum of the radial pressure wave registered by the hydrophones for a laser pulse with an energy of 7 mJ and a pulse duration of 10 ns (red), 15.6 ps (blue) and 780 fs (green). Dotted line, dashed line and continuous line correspond respectively to the low frequency, medium frequency and high frequency hydrophones.

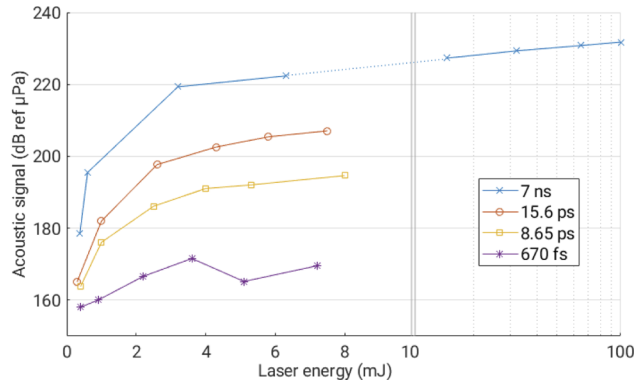


Fig. 3. Maximum amplitude of the acoustic signal measured in the middle frequency range (10 kHz-800 kHz) as a function of the laser pulse energy for laser pulse with durations of 7 ns (blue curve), 15 ps (red curve), 8 ps (yellow curve) and 670 fs (violet curve).

3.3. Effect of the laser repetition rate

To analyze possible cumulative effects from the laser on the shockwave generation, we investigated the influence of the laser repetition rate on the acoustic signal. Though the used pump lasers can work at 10 Hz, the repetition rate was reduced to 0.1 Hz in previous measurements to avoid such cumulative effects. Indeed, due to the formation of cavitation bubbles that can last for milliseconds [27], the laser propagation can be perturbed at high repetition rates by the presence of bubbles formed by the previous pulse. This effect is clearly observed with the ps and fs laser pulses, where the acoustic signal decreases when laser repetition rate was increased (Fig. 4). Surprisingly, the signal amplitude for ns pulses has opposite trend, since the pressure wave amplitude increases by 15% when the repetition rate is increased from 0.1 Hz to 10 Hz. In this case the laser peak power (1.3 MW) is too low for self-focusing and concomitant shift of the focus, and energy deposition is only possible at the focus. Therefore the beam is not perturbed before

Optics EXPRESS

the geometrical focus by previously formed bubbles. Remaining bubbles or inhomogeneities left at the focus can instead serve as a trigger for avalanche ionization of subsequent pulses.

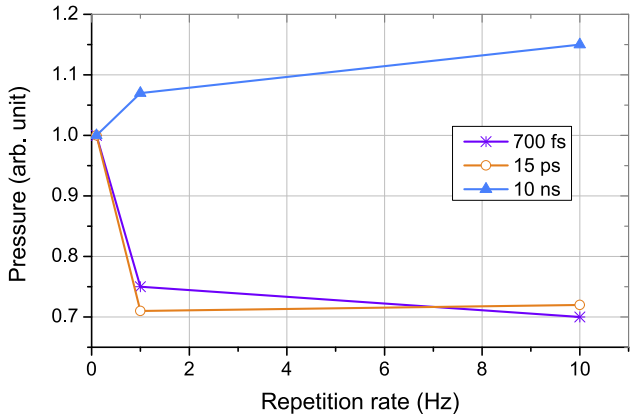


Fig. 4. Signal dependence on the laser repetition rate for three pulse durations: 670 fs 33 mJ (violet curve), 15.6 ps 44 mJ (orange curve), 10 ns 13 mJ (blue curve). The signal is normalized to the value at 0.1 Hz.

3.4. *Propagation of the pressure wave*

Finally, the shape of the acoustic wave produced by the laser has been measured using a time-resolved Schlieren technique (see description in Ref. [28]). A low intensity probe nanosecond laser beam was sent perpendicularly to the pump laser path in the water tank (see Fig. 1). The slight index variations produced by the acoustic waves in the medium are registered by the wavefront of the probe beam, which is monitored by a synchronized MCP detector with ns gate time. By changing the delay between the pump laser pulse and the probe beam, one can reconstruct the evolution of the shape of the acoustic wave as shown in Fig. 5. Measurements were done at three different delays after the plasma formation (namely 100 ns, 500 ns and 1000 ns) and the spatial resolution was about 30 µm. The parameters of the laser were the same as in Fig. 3. With the femtosecond laser pulse, the generated shock wave has a cylindrical shape, in agreement with the observations made in [4]. The pressure wave generated by the 15 ps pulse is also cylindrical but is much stronger. Close inspection of the images show that this cylindrical wave is the superposition of closely spaced tiny spherical waves emitted along the laser propagation axis. Finally, in the case of nanosecond laser pulse, the shock wave is even more contrasted and its shape is perfectly spherical. These observations are confirmed by measurement of the decay of the acoustic pressure as a function of distance from the source, presented in Fig. 6(a). For ns pulse with energy in excess of 10 mJ we observe the formation of several sources aligned along the axis and the corresponding distortion of the spherical acoustic wave into an elliptical wave. Such apparition of multiple breakdown has already been described in Ref. [29]. As expected the spherical source pressure amplitude has a decay law in the form of $1/r$ ($1/r^2$ for the energy) in contrast to a slower decay for the cylindrical source. Finally, the directivity of the pressure wave was measured along the z axis 8 cm away from the laser propagation axis. $z = 0$ corresponds to the laser geometrical focus. It confirms that the source produced by the picosecond laser is more directive than the one produced by the nanosecond laser (see Fig. 6(b)).

Optics EXPRESS

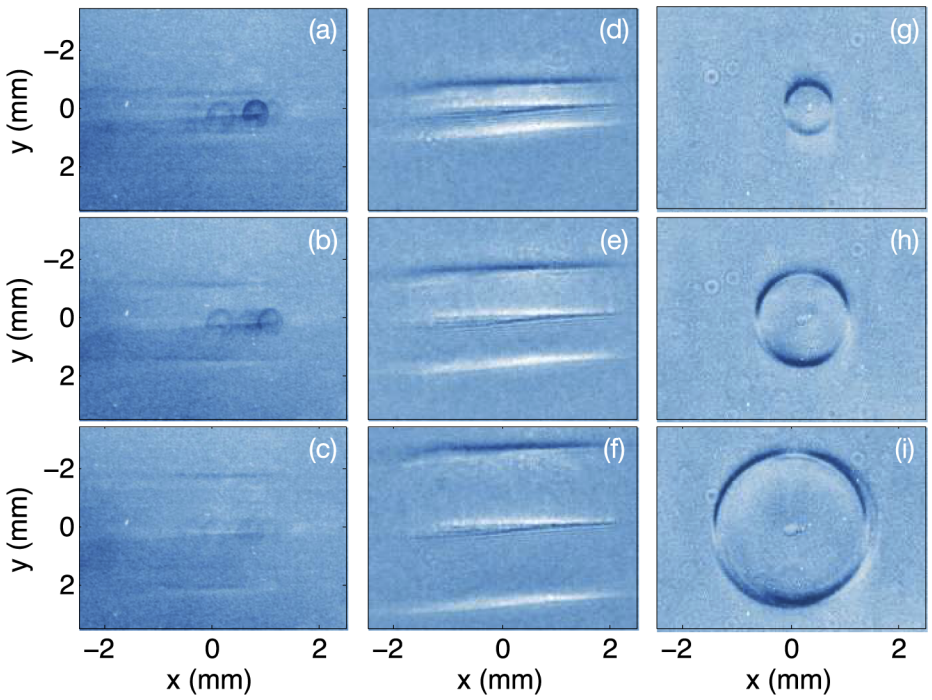


Fig. 5. (a) Schlieren images of the temporal evolution of the acoustic wave produced by a laser pulse of 7 mJ energy with a pulse duration of 700 fs (left), 15 ps (centre) et 10 ns (right). Images are made after a delay of 200 ns (a, d, g), 500 ns (b, e, h) and 1 µs (c, f, i) with respect to the pump laser pulse.

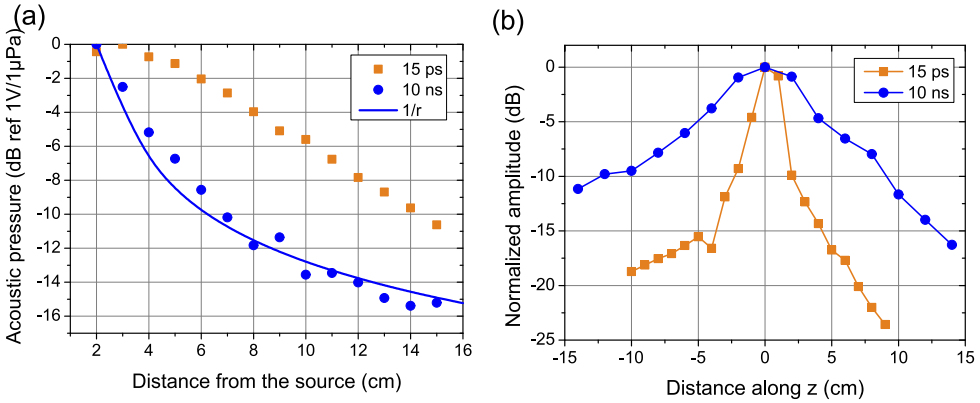


Fig. 6. (a) Evolution of the amplitude of the pressure wave recorded by the high frequency hydrophone as a function of the distance from the source. 1/r and $1/r^{1/2}$ decays are also presented for comparison. (b) Directivity of the pressure wave measured along z axis at a distance of 8 cm from the laser propagation axis. $z = 0$ corresponds to the laser focus.

Optics EXPRESS

4. Numerical simulations

To understand the effect of the laser pulse duration we have performed numerical simulations of the laser pulse propagation and deposition of energy. The pulse energy was fixed to 8.5 mJ while the pulse duration was changed by introduction of a phase modulation. Simulations were performed under the assumption of a constant pulse duration. We have calculated the deposited energy density and estimated the laser-matter interaction volume from the estimated beam radius obtained by second order moments as in Ref. [23]. The calculated fluence profiles obtained for three characteristic pulse durations are presented in Fig. 7. On can observe in the case of the fs pulse, the apparition of small scale filamentation several centimeters before and after the geometrical focus. The resulting energy deposition is spread over a large volume as shown in Ref. [23], in contrast with the propagation of the nanosecond pulse, whose peak power is too low to induce self-focusing and that can therefore create a millimeter scale breakdown.

The calculated deposited energy density for different pulse durations is presented in Fig. 8. As the pulse duration increases, we observe an increase of the maximum deposited energy density correlated with a reduction of multifilamentation and a contraction of the deposited energy volume. For comparison, the maximum pressure amplitude as a function of the laser input pulse duration is also presented, showing a very similar evolution to the calculated energy density. These results are in good agreement with the acoustic pressures reported in Ref. [5] for ps and ns laser pulse durations.

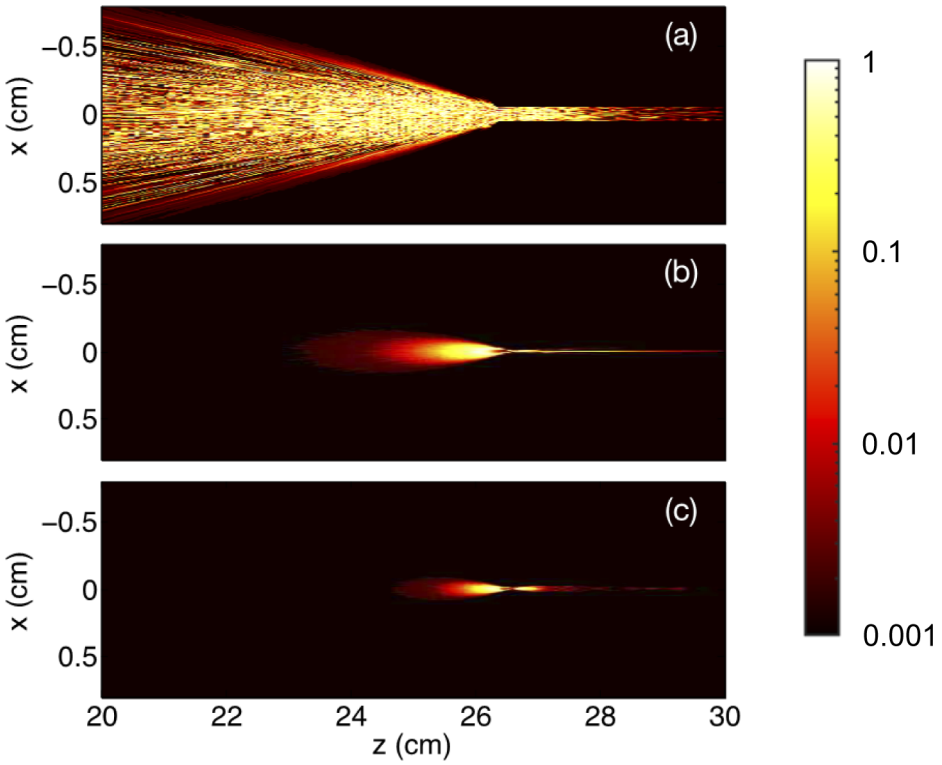


Fig. 7. Calculated fluence distribution for a laser pulse 8.5 mJ of 700 fs (a), 13 ps (b) and 10 ns (c) pulses propagating in water. Normalized fluence is presented in logarithmic scale with a normalization factor of 4.2 J/cm^2, 45.5 J/cm^2 and 6*10^4 J/cm^2 for 700 fs, 13 ps, and 10 ns pulse duration respectively.

Optics EXPRESS

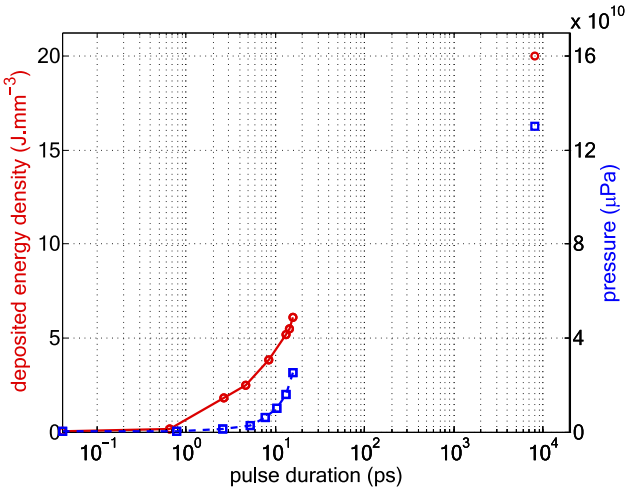


Fig. 8. Measured maximum amplitude of the pressure wave as a function of the laser pulse duration (blue curve) and calculated deposited energy density on the axis for the same laser pulse parameters (red curve).

5. Conclusion

We have performed experiments to analyze the influence of the laser pulse duration and energy on the generation of pressure waves in water. Spectrum analysis shows that a very broad acoustic wave spectrum is generated in every case and that the low frequency component is enhanced with nanosecond pulse duration. We have observed a nonlinear dependence of the pressure wave maximum on pulse duration and pulse energy. While femtosecond and picosecond pulses generate an elongated acoustic source through filamentation, nanosecond pulses generate pressure waves at least 20 dB higher than ps and fs laser in the sub-MHz domain. The highest pressure signal has been obtained with the laser with a 10 ns pulse duration and energy of a few mJ yielding a signal of 240 dB ref 1µPa in the frequency range 10 kHz-10 MHz. The Schlieren images of the pressure wave showed that for a laser pulse energy of 5 mJ, nanosecond pulses generate spherical waves while picosecond and fs pulses generate cylindrical waves. With higher nanosecond pulse energies the acoustic emission becomes more and more cylindrical and consequently the pressure wave is enhanced in the direction perpendicular to the laser axis.

Funding. Direction Générale de l'Armement (1783000801).

Disclosures. The authors declare no conflicts of interest.

Data availability. Data underlying the results presented in this paper are not publicly available at this time but may be obtained from the authors upon reasonable request.

References

1. P. K. Kennedy, D. X. Hammer, and B. A. Rockwell, "Laser-induced breakdown in aqueous media," Prog. Quantum Electron. **21**(3), 155–248 (1997).
2. J. Noack and A. Vogel, "Laser-induced plasma formation in water at nanosecond to femtosecond time scales: calculation of thresholds, absorption coefficients, and energy density," IEEE J. Quantum Electron. **35**(8), 1156–1167 (1999).
3. F. V. Potemkin, E. I. Mareev, A. A. Podshivalov, and V. M. Gordienko, "Laser control of filament-induced shock wave in water," Laser Phys. Lett. **11**(10), 106001 (2014).
4. Y. Brelet, A. Jarnac, J. Carbonnel, Y.-B. André, A. Mysyrowicz, A. Houard, D. Fattaccioli, R. Guillermin, and J.-P. Sessarego, "Underwater acoustic signals induced by intense ultrashort laser pulse," J. Acoust. Soc. Am. **137**(4), EL288–EL292 (2015).
5. J. Yellaiah and P. Prem Kiran, "Input pulse duration effect on laser-induced underwater acoustic signals," Appl. Opt. **60**(16), 4582 (2021).

Optics EXPRESS

6. L. V. Wang, "Ultrasound-mediated Biophotonic Imaging: A Review of Acousto-optical Tomography and Photoacoustic Tomography," Disease Markers **19**(2-3), 123–138 (2004).
7. A. Taruttis and V. Ntziachristos, "Advances in real-time multispectral optoacoustic imaging and its applications," Nat. Photonics **9**(4), 219–227 (2015).
8. L. V. Wang and S. Hu, "Photoacoustic Tomography: In Vivo Imaging from Organelles to Organs," Science **335**(6075), 1458–1462 (2012).
9. P. Beard, "Biomedical photoacoustic imaging," Interface Focus. **1**(4), 602–631 (2011).
10. S. V. Egerev, "In search of a noncontact underwater acoustic source," Acoust. Phys. **49**(1), 51–61 (2003).
11. T. G. Jones, M. K. Hornstein, and A. C. Ting, "Intense underwater laser acoustic source for Navy applications," J. Acoust. Soc. Am. **125**(4), 2556 (2009).
12. A. Vogel, S. Busch, and U. Parlitz, "Shock wave emission and cavitation bubble generation by picosecond and nanosecond optical breakdown in water," J. Acoust. Soc. Am. **100**(1), 148–165 (1996).
13. D. Ristau, *Laser-Induced Damage in Optical Materials* (CRC press, Taylor &Francis Group, Florida, 2014).
14. X. Liu, D. Du, and G. Mourou, "Laser ablation and micromachining with ultrashort laser pulses," IEEE J. Sel. Top. Quant. Electron. **33**(10), 1706–1716 (1997).
15. R. R. Gattass and E. Mazur, "Femtosecond laser micromachining in transparent materials," Nat. Photonics **2**(4), 219–225 (2008).
16. V. Garzillo, V. Jukna, A. Couairon, R. Grigutis, P. Di Trapani, and O. Jedrkiewicz, "Optimization of laser energy deposition for single-shot high aspect-ratio microstructuring of thick BK7 glass," J. Appl. Phys. **120**(1), 013102 (2016).
17. D. Strickland and G. Mourou, "Compression of Amplified Chirped Optical Pulses," Opt. Commun. **55**(6), 447–449 (1985).
18. C. Herkommer, P. Krötz, R. Jung, S. Klingebiel, C. Wandt, R. Bessing, P. Walch, T. Produit, K. Michel, D. Bauer, R. Kienberger, and T. Metzger, "Ultrafast thin-disk multipass amplifier with 720 mJ operating at kilohertz repetition rate for applications in atmospheric research," Opt. Express **28**(20), 30164 (2020).
19. A. Houard, V. Jukna, G. Point, Y.-B. André, S. Klingebiel, M. Schultze, K. Michel, T. Metzger, and A. Mysyrowicz, "Study of filamentation with a high power high repetition rate ps laser at 1.03 μm," Opt. Express **24**(7), 7437 (2016).
20. M. H. Helle, T. G. Jones, J. R. Peñano, D. Kaganovich, and A. Ting, "Formation and propagation of meter-scale laser filaments in water," Appl. Phys. Lett. **103**(12), 121101 (2013).
21. F. V. Potemkin, E. I. Mareev, A. A. Podshivalov, and V. M. Gordienko, "Highly extended high density filaments in tight focusing geometry in water: from femtoseconds to microseconds," New J. Phys. **17**(5), 053010 (2015).
22. G. Point, Y. Brelet, A. Houard, V. Jukna, C. Milian, J. Carbonnel, Y. Liu, A. Couairon, and A. Mysyrowicz, "Superfilamentation in Air," Phys. Rev. Lett. **112**(22), 223902 (2014).
23. V. Jukna, A. Jarnac, C. Milián, Y. Brelet, J. Carbonnel, Y.-B. André, R. Guillermin, J.-P. Sessarego, D. Fattaccioli, A. Mysyrowicz, A. Couairon, and A. Houard, "Underwater acoustic wave generation by filamentation of terawatt ultrashort laser pulses," Phys. Rev. E **93**(6), 063106 (2016).
24. R. Petkovšek and P. Gregorčič, "A laser probe measurement of cavitation bubble dynamics improved by shock wave detection and compared to shadow photography," J. Appl. Phys. **102**(4), 044909 (2007).
25. C. E. Brenner, "Cavitation and Bubble Dynamics," Oxford University Press, New York, 1995.
26. W. Kuperman and P. Roux, (2007) Underwater Acoustics, In: T Rossing, ed. *Springer Handbook of Acoustics. Springer Handbooks*. Springer, New York, NY.
27. D. Faccio, G. Tamošauskas, E. Rubino, J. Darginavičius, D. G. Papazoglou, S. Tzortzakis, A. Couairon, and A. Dubietis, "Cavitation dynamics and directional microbubble ejection induced by intense femtosecond laser pulses in liquids," Phys. Rev. E **86**(3), 036304 (2012).
28. P.-Q. Elias, N. Severac, J.-M. Luyssen, Y.-B. André, I. Doudet, B. Wattellier, J.-P. Tobeli, S. Albert, B. Mahieu, R. Bur, A. Mysyrowicz, and A. Houard, "Improving supersonic flights with femtosecond laser filamentation," Sci. Adv. **4**(11), eaau5239 (2018).
29. L. Fu, S. Wang, J. Xin, S. Wang, C. Yao, Z. Zhang, and J. Wang, "Experimental investigation on multiple breakdown in water induced by focused nanosecond laser," Opt. Express **26**(22), 28560 (2018).

147.250.2.201 {ts '2022-03-07 09:56:56'}